Journal of Information Systems Engineering and Management
2024, 9(4)
e-ISSN: 2468-4376
https://www.jisem-journal.com/

Research Article

Metaheuristic Optimization Algorithm Based Multi Objective Optimal Power Flow Incorporating Generator Reallocation and Facts Device Integration for Voltage Stability Improvement and Loss Reduction

J. Ayyappa[1*], Dr. N. Jayakumar[2], Dr. A. Srinivasa Reddy[3]
[*1]Research Scholar, Department of Electrical and Electronics Engineering, Annamalai University, Annamalai Nagar, Chidambaram, Tamil Nadu, India
and
Assistant Professor, Department of Electrical and Electronics Engineering, Sir C R Reddy College of Engineering, Eluru, Andhra Pradesh, India
Email: ayyappacrr@gmail.com
[2]Assistant Professor, (Deputed from Annamalai University) Lecturer, Dept. of EEE Government Polytechnic College, Ariyalur. Tamil Nadu, India.
Email: jayakumar_382@yahoo.co. in
[3] Professor & HOD, EEE Dept., Sir C. R. Reddy College of Engineering, Eluru, India.

ARTICLE INFO

Received: 10 Oct 2024
Accepted: 24 Nov 2024

ABSTRACT

Efficient operation of power systems requires minimizing energy losses, maintaining voltage stability, and ensuring secure power transfer within operational boundaries. This paper formulates an OPF model that jointly considers generation cost, active power losses, voltage deviation, and generator reallocation as key objectives. The HHO algorithm, inspired by cooperative hunting behaviour, is employed to solve the multi-objective OPF problem on the IEEE 30-bus and 57-bus benchmark networks. To assess system resilience, contingency analysis is conducted under severe outage conditions, highlighting vulnerable locations where corrective actions are most effective. In addition, three FACTS devices UPFC, TCSC, and SVC are integrated, with their placement determined using a HI for congestion mitigation and voltage support. Simulation outcomes demonstrate that HHO achieves superior performance compared to the GA in terms of convergence speed, robustness, and solution accuracy. The findings confirm that incorporating generator reallocation and FACTS controllers significantly enhances network reliability and operational efficiency.

Keyword: Optimal Power Flow (OPF), Harris Hawks Optimization (HHO), Genetic Algorithm (GA), Flexible AC Transmission Systems (FACTS), Unified Power Flow Controller (UPFC), Thyristor Controlled Series Capacitor (TCSC), Static Var Compensator (SVC), Hybrid Index (HI).

INTRODUCTION

The reliable, economic, and secure operation of today's power systems is becoming increasingly difficult because of rising demand, higher interconnection levels, and tighter operating margins. OPF has emerged as a fundamental tool to tackle these challenges, as it determines optimal generator dispatch, voltage set points, and power flows while minimizing cost and losses under engineering and operational constraints.

Classical OPF Approaches: The OPF problem was first formulated by Dommel and Tinney (1968) [14], laying the groundwork for combining economic objectives with technical requirements. Conventional solvers such as Newton–Raphson, interior-point, and sequential quadratic programming were extensively applied to convex OPF models, offering good convergence. However, their dependence

Research Article

on derivative information restricted their use in practical systems, where non convexities such as valve point effects, discrete control devices, and prohibited zones are common. Later studies, such as Chang and Huang (1998) [11], which investigated reactive power margins, and Gao et al. (1992) [18], which focused on modal analysis, extended OPF applications to include system stability considerations.

FACTS Devices in OPF: The introduction of FACTS provided new opportunities for enhancing controllability and efficiency. Galiana et al. (1996) [20] outlined the benefits of FACTS, while Gotham and Heydt (1998) [21] discussed their integration in power flow models. Research subsequently shifted toward the allocation of devices: Jurado and Rodriguez (1999) [24] studied SVC siting under contingencies, and Gerbex et al. (2001) [19] applied Genetic Algorithms (GA) for multi-device placement. More recent studies, such as Aghaei et al. (2012) [1] and Belyaev et al. (2015) [8], demonstrated how optimal FACTS allocation enhances reliability and reduces transmission losses. El-Azab et al. (2020) [15] further advanced this by considering probabilistic uncertainties and dynamic line ratings, bringing models closer to real-world practice.

Rise of Metaheuristic Optimization: The shortcomings of gradient based solvers encouraged the adoption of metaheuristic algorithms for OPF. Goldberg (1989) [13] introduced the GA, which Bakirtzis et al. (2002) [7] successfully applied to OPF. Later, Cui-Ru Wang et al. (2005) [12] enhanced Particle Swarm Optimization (PSO), while Ela et al. (2010) [16] validated Differential Evolution (DE) for non-convex OPF. Geem et al. (2001) [17] developed the Harmony Search (HS) method, which also proved effective in OPF contexts. Swarm intelligence techniques, such as those studied by Bhattacharyya and Raj (2016) [9] and refined by Bhattacharyya and Karmakar (2020) [10], demonstrated strong capability in managing nonlinear power system constraints.

Hybrid and modified algorithms have also been explored. Rajan and Malakar (2015) [5] combined the Firefly Algorithm with Nelder–Mead for reactive power dispatch, while Shaheen et al. (2017) [6] applied the Backtracking Search Algorithm (BSA) for fast and reliable OPF solutions. FACTS-focused optimization also gained momentum: Kumar and Kalavathi (2014) [26] used Cat Swarm Optimization for UPFC placement, and Kumar and Srikanth (2015) [27] developed hybrid optimization frameworks for UPFC allocation. In addition, Kazemi and Badrzadeh (2004) [28] modeled SVC and TCSC operation at load ability limits, providing insights for device coordination. In recent years, nature-inspired algorithms have been widely adopted. Heidari et al. (2019) [30] introduced Harris Hawks Optimization (HHO), which balances exploration and exploitation to effectively solve non-convex OPF problems. Santhosh and Neela (2021) [29] applied HHO for microgrid optimization with distributed generation, showing notable improvements in efficiency. Jayasankara et al. (2010) [23] developed neural-network-based stability indices for TCSC allocation, and Krishnan and McCalley (2012) [25] proposed risk-based contingency frameworks.

FACTS Placement and Index Guided Optimization: The effectiveness of FACTS depends strongly on their placement. Widely used devices include the UPFC, TCSC, and SVC. Placement is often guided by indices such as the L-index for bus voltage stability, the Fast Voltage Stability Index (FVSI) for line margins, and the Line Utilization Factor (LUF) for congestion levels. While single-index methods are simple, they may produce biased results. Hybrid index-based methods, on the other hand, yield more balanced outcomes. Several studies integrating FACTS with metaheuristics like GA, PSO, and DE have reported reductions in power losses and voltage deviations. For larger networks such as IEEE 57-bus and 118-bus, newer optimizers consistently outperform GA in both robustness and convergence.

Contingency Analysis in Secure OPF: Alongside optimization, contingency analysis is essential for ensuring secure operations. N–1 contingency evaluation, which considers the failure of individual generators or lines, remains a standard practice. Efficient approximations are often used for screening, with results validated by full AC power flow studies. When combined with FACTS placement and hybrid indices, contingency analysis enhances post-fault stability, alleviates overloads, and strengthens overall resilience, making it a vital part of modern OPF research.

Journal of Information Systems Engineering and Management
2024, 9(4)
e-ISSN: 2468-4376
https://www.jisem-journal.com/

Research Article

Integrated HHO-Based Secure OPF with FACTS and Contingency Analysis: Building on these advancements, the HHO algorithm drawing inspiration from cooperative hunting strategies has been applied to solve multi-objective OPF on IEEE 30-bus and 57-bus networks. To evaluate system resilience, contingency analysis under severe outages is conducted to identify vulnerable points where corrective actions are most effective. Furthermore, three FACTS devices (UPFC, TCSC, and SVC) are incorporated, with their placement determined by a Hybrid Index (HI) that addresses both congestion relief and voltage support. Results show that HHO outperforms GA in convergence speed, accuracy, and robustness. The findings also confirm that combining generator reallocation with FACTS controllers substantially improves system reliability and operational efficiency.

1. PROPOSED FACTS DEVICES PLACEMENT INDICES

In this work, the Hybrid Index (HI) is computed by combining the Line Utilization Factor (LUF) and the Fast Voltage Stability Index (FVSI) with equal weighting, where Z1=0.5 and Z2=0.5. The LUF (S1) measures how much of a transmission line's capacity is being used, while the FVSI (S2) indicates the line's proximity to voltage instability. By giving equal importance to both factors, the HI provides a balanced assessment of stressed transmission lines, making it suitable for determining TCSC placement. The effectiveness of FACTS controllers depends heavily on their location, which is guided by voltage stability and congestion indices. The L-index is widely used to evaluate bus voltage stability, with higher values indicating weaker buses that require reactive power support. Therefore, the SVC is installed at buses with high L-index values to improve voltage profiles. For the UPFC, both the L-index and HI are used together because it can simultaneously regulate bus voltages and control line flows. This integrated placement strategy ensures that each FACTS device effectively contributes to voltage stability improvement, loss reduction, and congestion management.

$$L\_\text{index}\ (L_I) = \left|1 - \sum_{i=1}^{g} F_{ji} \frac{V_i}{V_j}\right| \quad (1)$$

$$HI = Z_1 \times S_1 + Z_2 \times S_2 \quad (2)$$

$$S_1 = \frac{MVAij}{MVAij^{max}} \quad (3)$$

$$S_2 = 4\frac{Z^2 Qj}{Vi^2 X} \quad (4)$$

2. PROBLEM FORMULATION

For effective generator tuning, a multi-objective optimization framework is adopted, considering fuel cost, active power losses, and voltage profile deviations. The objective function is expressed as:

$$Min\ F = Min\ (W1 * F1 + W2 * F2 + W3 * F3) \quad (5)$$

where W_1, W_2, W_3 are the weighting factors assigned to fuel cost, voltage deviation, and real power losses, respectively.

For this study, the chosen values are:

$W_1+W_2+W_3=1$

$W_1=0.15$, $W_2=0.7$, $W_3=0.15$

Voltage deviation is minimized to ensure a secure and stable operating condition of the system:

$$\text{F1=min (VD)}=min\left(\sum_{k=1}^{Nbus} \left(V_K - S_k^{ref}\right)^2\right) \quad (6)$$

The total active power losses in the transmission lines are given by:

$$\text{F2}=min\left(\sum_{i=1}^{ntl} real\left(S_{jk}^i + S_{kj}^i\right)\right)$$

(7)

The fuel cost of thermal generating units is modelled as a quadratic function of generator output:

Journal of Information Systems Engineering and Management
2024, 9(4)
e-ISSN: 2468-4376
https://www.jisem-journal.com/

Research Article

$$F3 = min\left(\sum_{i=1}^{ng} \quad (a_i + b_i P_{Gi} + C_i P_{Gi}^2)\right)$$
(8)

Equality constraints:

Power Balance Constraint

$$\sum_{i=1}^{N} P_{Gi} = \sum_{i=1}^{N} P_{Di} + P_L \tag{9}$$

$$\sum_{i=1}^{N} Q_{Gi} = \sum_{i=1}^{N} Q_{Di} + Q_L \tag{10}$$

Inequality constraints:

Voltage balance constraint

$$V_{Gi}\min \le V_{Gi} \le V_{Gi}\max \tag{11}$$

Real power generation limit:

$$P_{Gi}\min \le P_{Gi} \le P_{Gi}\max \tag{12}$$

Reactive Power generation limits:

$$Q_{Gi}\min \le Q_{Gi} \le Q_{Gi}\max \tag{13}$$

Modelling of UPFC

UPFC voltage sources are written in equations 14 & 15

$$V_{vR}(\cos\delta_{vR} + j\sin\delta_{vR}) \tag{14}$$

$$V_{cR}(\cos\delta_{cR} + j\sin\delta_{cR}) \tag{15}$$

The active and reactive power equations are,

At bus k

$$P_k = [V_k V_m B_{km} \sin(\theta_k - \theta_m)] + [V_k V_{cR} B_{km} \sin(\theta_k - \delta_{cR})] + [V_k V_{vR} B_{vR} \sin(\theta_k - \delta_{vR})] \tag{16}$$

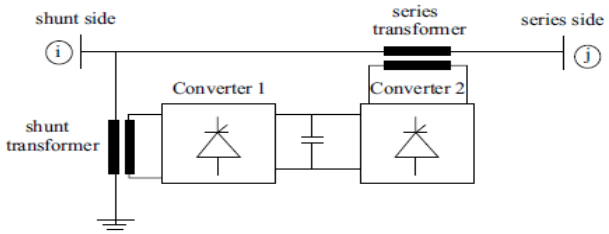

Figure.1. Schematic arrangement of the UPFC

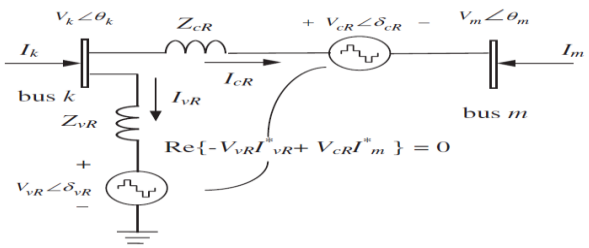

Figure.2 Equivalent circuit of the UPFC

Journal of Information Systems Engineering and Management
2024, 9(4)
e-ISSN: 2468-4376
https://www.jisem-journal.com/

Research Article

$$Q_k = -V_k{}^2\ B_{kk} - [V_k V_m B_{km}\ cos(\theta_k - \theta_m)] - [V_k V_{cR} B_{km}\ cos(\theta_k - \delta_{cR})] - [V_k V_{vR} B_{vR}\ cos(\theta_k - \delta_{vR})] \quad (17)$$

At bus m

$$P_m = [V_m V_k B_{mk}\ sin(\theta_m - \theta_k)] + [V_m V_{cR} B_{mm}\ sin(\theta_m - \delta_{cR})] \quad (18)$$

$$Q_m = -V_m^2 B_{mm} - [V_m V_k B_{mk}\ cos(\theta_m - \theta_k)] - [V_m V_{cR} B_{mm}\ cos(\theta_m - \delta_{cR})] \quad (19)$$

At Series converter:

$$P_{cR} = [V_{cR} V_k B_{km}\ sin(\delta_{cR} - \theta_k)] + [V_m V_{cR} B_{mm}\ sin(\delta_{cR} - \theta_m)] \quad (20)$$

$$Q_{cR} = -V_{cR}^2\ B_{mm} - [V_k V_{cR} B_{km}\ cos(\theta_k - \delta_{cR})] - [V_m V_{cR} B_{mm}\ cos(\theta_m - \delta_{cR})] \quad (21)$$

At Shunt converter:

$$P_{vR} = V_{vR} V_k B_{vr}\ \sin(\delta_{nR} - \theta_k) \quad (22)$$

$$Q_{vR} = V_{vR}^2 B_{vR} - V_{vR} V_k B_{vR}\ \cos(\delta_{vR} - \theta_k) \quad (23)$$

3. PROPOSED APPROACH

This work introduces a four step methodology to enhance the performance of power systems using two advanced optimization techniques: HHO and the GA. The primary objectives are to reduce power generation costs, minimize real power losses, and improve voltage stability under both normal and contingency conditions. The proposed framework is structured as follows:

Step 1: OPF without FACTS devices

In the first stage, the OPF problem is solved for the IEEE 30-bus test system without incorporating any FACTS devices. Both HHO and GA are applied to minimize generation cost, reduce losses, and enhance the system's voltage profile while adhering to operational constraints. The outcomes of this step establish a baseline for comparison.

Step 2: OPF with FACTS device integration

The second stage incorporates FACTS controllers into the system. Devices such as the UPFC, TCSC, and SVC are employed to regulate power flows, improve voltage stability, and alleviate congestion. The OPF is re-optimized using HHO and GA with these devices in place, and the results are compared with Step 1 to evaluate improvements in system performance.

Step 3: Contingency analysis without FACTS devices

In the third stage, an N-1 contingency analysis is carried out to assess system reliability under unexpected events, such as the outage of a transmission line. Both HHO and GA are applied to optimize OPF under these stressed conditions, emphasizing voltage stability and loss minimization. This step is executed without FACTS devices, providing insights into the vulnerability of the system during contingencies.

Step 4: Contingency Analysis with Integrated FACTS Devices

After installing the devices, the contingency cases are checked again to study their effect on system stability, power flow, and voltage profile. The placement of FACTS controllers is very important because their performance depends on location. The L-index is useful for SVC placement as it shows weak buses. The HI is suitable for TCSC placement as it combines line loading and voltage stability. For UPFC, both indices are used together because the device can control voltage as well as line flows. This approach makes sure that each FACTS device improves voltage stability, reduces losses, and manages congestion effectively.

Harris Hawks Optimization (HHO)

HHO is a population-based metaheuristic that relies on randomization, which means that its outcomes can differ from one execution to another. To obtain results that are both reliable and statistically meaningful, the algorithm is executed for 20 independent runs under identical parameter

Step 1: Initialization

- ✓ Generate random hawk positions (possible solutions).
- ✓ Identify the rabbit (best solution so far).

Step 2: Exploration Phase

Journal of Information Systems Engineering and Management
2024, 9(4)
e-ISSN: 2468-4376
https://www.jisem-journal.com/

Research Article

settings: a population size of 20, a maximum of 50 iterations, an initial energy value of 2, an escaping energy decay rate of 0.05, and a randomization probability of 0.3. After completing these runs, the results are assessed using four performance indicators. The best value corresponds to the lowest objective function recorded, representing the most optimal solution achieved. The mean value indicates the average solution quality across all runs, while the worst value highlights the maximum objective obtained, reflecting the least favourable outcome.

✓ If prey has high energy ($\|E\| \geq 1$) → hawks search widely. ✓ Hawks update positions randomly around the environment.
Step 3: Transition Condition Prey's energy decreases over iterations. When $\|E\| < 1$, the algorithm shifts from exploration to exploitation.
Step 4: Exploitation Phase Hawks use 4 attack strategies: 1. **Soft besiege** (slowly surround prey). 2. **Hard besiege** (direct fast attack). 3. **Soft besiege with dive** (encircle + sudden strike). 4. **Hard besiege with dive** (direct strike + sudden dive).
Step 5: Elitism Keep the best hawk (closest to prey).
Step 6: Termination When stopping condition is met → best hawk position = optimal solution.

Genetic Algorithm (GA):GA is an evolutionary optimization method based on the principle of natural selection. Candidate solutions are encoded as chromosomes and improved across generations through three operators: selection (choosing the fittest individuals), crossover (recombining parent solutions to create new offspring), and mutation (introducing small random changes to preserve diversity). This iterative process enhances solution quality, making GA well-suited for nonlinear and multi-objective OPF problems.

4. RESULTS AND DISCUSSION

From Figure 3, it is evident that bus 30 exhibits the maximum L-index value of 0.0891, supporting the findings obtained from the Newton–Raphson load flow study. The figure further illustrates that, in comparison with the remaining buses, bus 30 experiences a higher level of stress with respect to voltage stability, thereby identifying it as the most critical location in the system.

The analysis reveals that bus 30 is interconnected through the transmission lines 27–30 and 29–30. Among these, the HI assessment shows that the 27–30 line exhibits the highest severity, with a calculated value of 0.04324. Considering this outcome, a UPFC is strategically placed at bus 30 and along the 27–30 line to strengthen voltage stability and enhance the overall operational performance of the power system.

Journal of Information Systems Engineering and Management
2024, 9(4)
e-ISSN: 2468-4376
https://www.jisem-journal.com/

Research Article

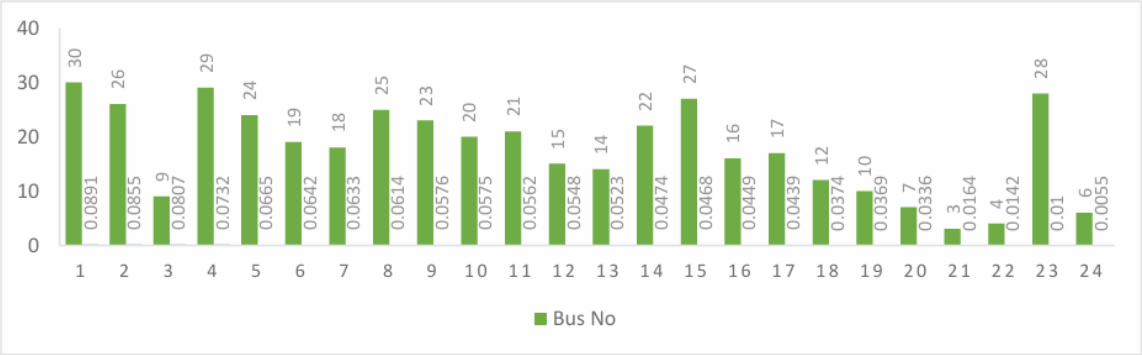

Figure 3 L-index values for the IEEE 30-bus system.

Table 2 presents the comparative results of the system performance with and without the UPFC using two optimization techniques, namely the GA and HHO. The table highlights variations in key parameters such as generation cost, active power losses, and voltage deviation under both scenarios. It is evident that the integration of the UPFC provides noticeable improvements in system performance for both algorithms. Moreover, the results show that HHO consistently achieves better optimization outcomes compared to GA, with lower cost, reduced losses, and improved voltage profiles. This demonstrates not only the effectiveness of the UPFC in enhancing system operation but also the superior search capability of HHO in handling the multi objective Optimal Power Flow problem.

Table 1. Generator Characteristics of IEEE 30-Bus System

Generator Bus No	a ($/MW²·hr)	b ($/MW·hr)	c ($/hr)	Pmin (MW)	Pmax (MW)
1	0.005	2.45	105	10	200
2	0.005	3.51	44.1	10	50
5	0.005	3.89	40.6	10	50
8	0.005	3.25	0	10	50
11	0.005	3	0	10	100
13	0.005	2.45	105	0	10

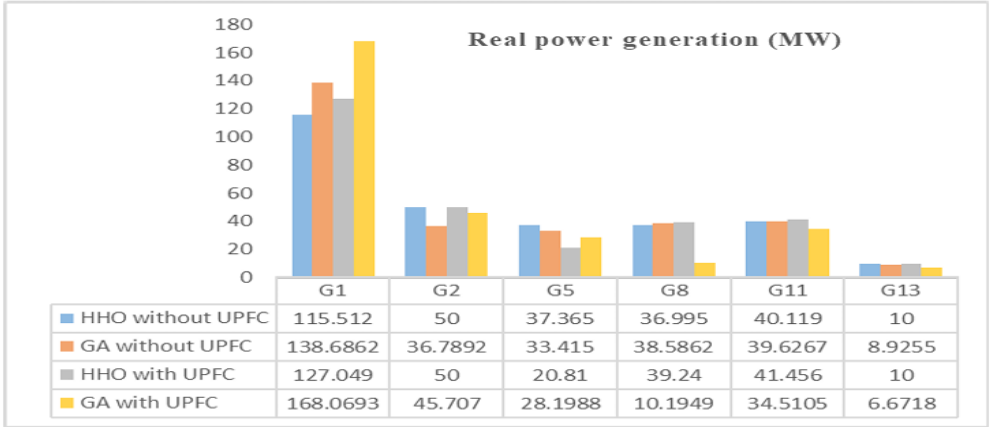

Figure 4. Generator output values with and without UPFC integration in the IEEE 30-bus system under normal operating conditions (no contingency).

Journal of Information Systems Engineering and Management
2024, 9(4)
e-ISSN: 2468-4376
https://www.jisem-journal.com/

Research Article

Table 2. (IEEE 30-bus, no contingency) comparing GA and HHO with/without UPFC

S.No	Parameter	HHO without UPFC	GA without UPFC	HHO with UPFC	GA with UPFC
1.	Real power generation	289.991	296	288.55	293.35
2.	Reactive power loss	15.898	35.35	4.462	25.14
3.	Voltage deviation(p.u.)	1.8355	2.5013	0.286	0.2859
4.	Active losses (MW)	6.591	12.6	5.15	9.95
5.	Fuel Cost ($/h)	1355.32	1366.9	1250.2	1260

Under the N−1 contingency condition resulting from the outage of the 27–28 transmission line, the power system experiences a noticeable decline in voltage stability. During this event, bus 30 registers a relatively high L-index value of 0.4522, identifying it as the most critical bus with respect to stability margin. Furthermore, the 27–30 line, which is directly linked to bus 30, records a HI of 0.1869, indicating its vulnerability under this contingency. These results emphasize the importance of applying corrective strategies, such as the optimal placement of a UPFC, to counteract the negative impact of the outage and reinforce overall system reliability and stability.

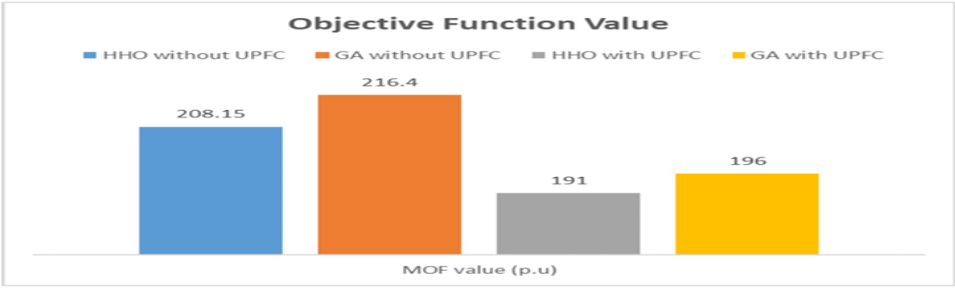

Figure 5: Multi-Objective Values under no contingency, with and without UPFC

Table 3. HHO-Based OPF with and without UPFC during Line 27–28 Contingency:

Parameter	HHO & GA Comparison			
	HHO without UPFC	GA without UPFC	HHO with UPFC	GA with UPFC
Total Real power generation (MW)	293.166	301.3267	290.6094	296.11
Total reactive power loss (MVAR)	26.16	39.24	8.16	27.14
Voltage deviation (p.u)	3.4022	3.9628	0.4099	0.4194
Active losses (MW)	9.766	17.9267	7.20944	12.71
Fuel cost ($/h)	1374.91	1380	1254.4	1272

Journal of Information Systems Engineering and Management
2024, 9(4)
e-ISSN: 2468-4376
https://www.jisem-journal.com/

Research Article

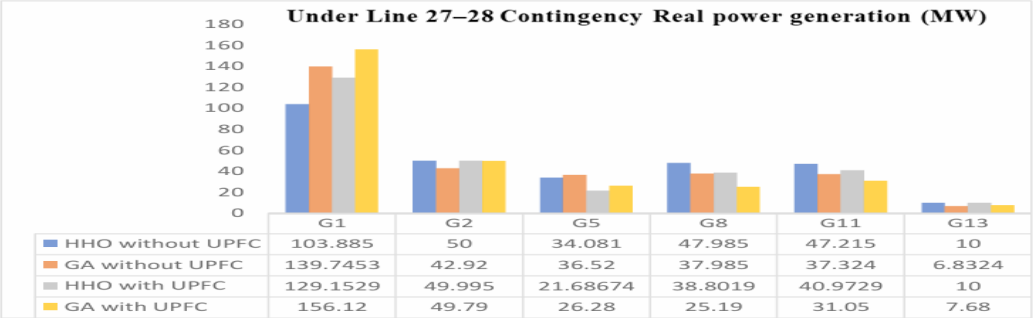

Figure 6. Real Power Generation under Contingency Conditions

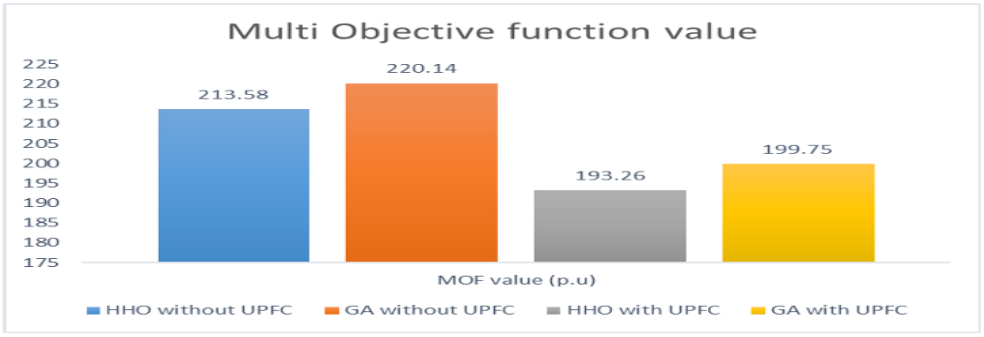

Figure 7. Multi-Objective Function Values under Contingency

In the IEEE 30-bus network, the UPFC operates in the normal state with a series voltage of 0.02 ∠ −85.01° pu and a shunt voltage of 1.005 ∠ −15.34° pu, which provides sufficient compensation to regulate bus voltages and maintain secure power transfer without stressing the converters. When a contingency occurs, the HHO algorithm identifies superior control settings, raising the series injection to 0.04 ∠ −87.12° pu and adjusting the shunt voltage to 1.0148 ∠ −20.91° pu, which strengthens corrective support, reduces real power losses, and improves voltage stability.

In the IEEE 30-bus system, the SVC is rated at 0.0687 ∠ −83.45° pu under normal operating conditions. At this level, the device provides moderate reactive power support, maintaining bus voltage stability and enabling smooth power transfer without stressing the system. During a contingency, the rating rises to 0.1732 ∠ −88.12° pu, which enhances reactive compensation, suppresses voltage deviations, and supports faster post-fault recovery.

IEEE 57-Bus System Performance with UPFC

The generator cost coefficients for the IEEE 57-bus system, provided in Table 4, are based on a 100 MVA system base. In the IEEE 57-bus system, the voltage stability assessment reveals that bus 31 exhibits the highest L-index value of 0.3836, identifying it as the weakest bus in the network. Bus 31 is directly connected to the 30–31 transmission line, which records a HI of 0.0617. Based on these findings, the optimal location for a UPFC is determined to be at bus 31 and along the 30–31 line, ensuring improved voltage stability and enhanced system performance. Under the N–1 contingency condition caused by the outage of the 11–43 transmission line, the system experiences severe voltage instability. In this scenario, bus 42 records the highest L-index value of 0.9556, identifying it as the most critical bus in the network. Furthermore, the 56–42 transmission line, which is directly connected to bus 42, exhibits a HI of 0.5926,

Journal of Information Systems Engineering and Management
2024, 9(4)
e-ISSN: 2468-4376
https://www.jisem-journal.com/

Research Article

Table 4. Generator Cost Coefficients for the IEEE 57-Bus System

Generator Bus No	a ($/MW²·hr)	b ($/MW·hr)	c ($/hr)	Pmin (MW)	Pmax (MW)
1	0.0775	20	0	0	575
2	0.01	40	0	0	100
3	0.25	20	0	0	140
6	0.1	40	0	0	100
8	0.02222	20	0	0	550
9	0.01	40	0	0	200
12	0.32258	20	0	0	410

Table 5. HHO-OPF, with and without UPFC for the IEEE 57 bus system under normal conditions.

Parameters	HHO without UPFC	HHO with UPFC at bus 31 and line 30-31
G1(MW)	252	245
G2(MW)	78	43
G3(MW)	65	85
G6(MW)	72	82
G8(MW)	466	498
G9(MW)	200	200
G12(MW)	109	85
Total real power generation (MW)	1243	1240
Fuel cost ($/hr)	46328	45880
Active losses (MW)	47	44.762
Voltage deviation (p.u)	5.7	3.085
MOF	6983	6913.7

confirming it as a highly vulnerable element. Based on these results, the optimal placement of the UPFC is determined at bus 42 and along the 56–42 line to mitigate instability and enhance system reliability. Table 6 shows the HHO-based OPF results for the 11–43 line outage scenario with and without UPFC installed at bus 42 and line 56–42. The integration of UPFC significantly reduces voltage deviation and active losses while lowering the fuel cost. Additionally, total real power generation is slightly decreased, and the multi-objective function (MOF) value improves, indicating enhanced system stability and economic performance under contingency conditions.

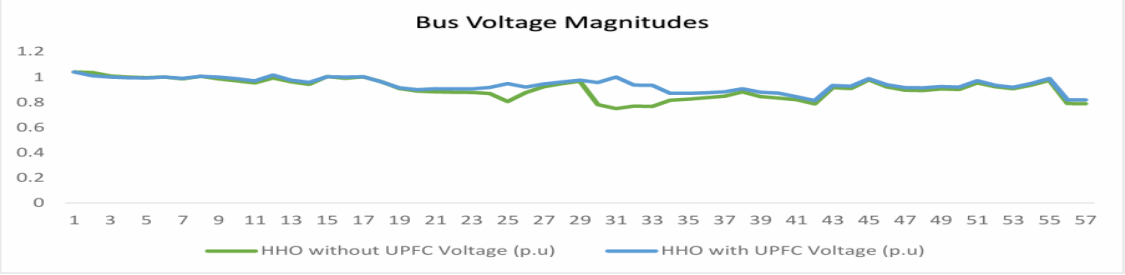

Figure 8. Voltage magnitude profile of the IEEE 57-bus system with and without UPFC

Journal of Information Systems Engineering and Management
2024, 9(4)
e-ISSN: 2468-4376
https://www.jisem-journal.com/

Research Article

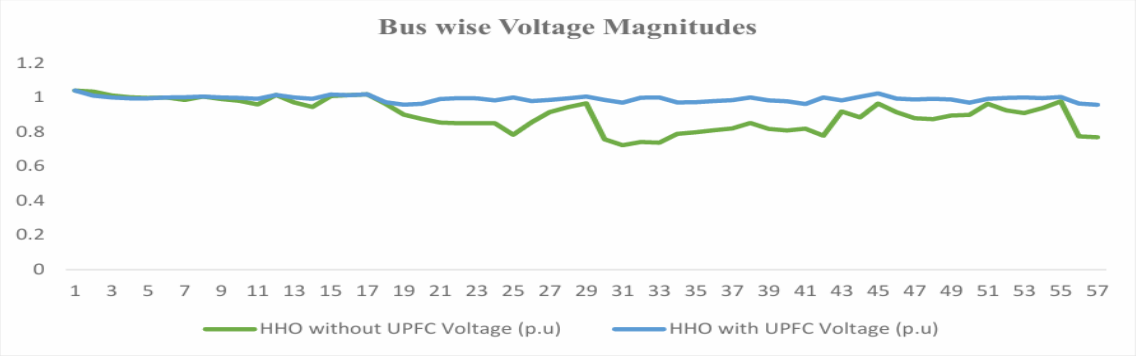

Figure 9. Voltage magnitude profile of the IEEE 57-bus system under contingency conditions with UPFC

Table 6. HHO-OPF for 11-43 (Line outage) with and without UPFC, UPFC is located at bus 42 and line 56-42.

Parameters	HHO without UPFC	HHO with UPFC bus 42 and line 56-42
G1(MW)	575	292
G2(MW)	100	37
G3(MW)	84	78
G6(MW)	9	78
G8(MW)	78	469
G9(MW)	200	200
G12(MW)	198	85
Total real power generation (MW)	1246.6	1241.03
Fuel cost ($/hr)	50285	48029
Active losses (MW)	50	45.23
Voltage deviation (p.u)	7.798	3.82
MOF	7579	7236

In the IEEE 57-bus system, the UPFC under normal operation is configured with $0.0861 \angle -84.75^\circ$ pu for series injection and $1.1068 \angle -14.85^\circ$ pu for the shunt converter, ensuring balanced operation and reliable power flow. Under contingency conditions, the HHO algorithm enhances these values to $0.1012 \angle -86.92^\circ$ pu and $1.1141 \angle -21.47^\circ$ pu, respectively, delivering stronger compensation, suppressing voltage deviations, minimizing system losses, and improving post-fault security. Thus, in both the 30-bus and 57-bus systems, the UPFC not only improves steady-state performance under normal operation but also, when optimally tuned during contingencies, significantly enhances grid resilience, operational reliability, and overall system efficiency.

SVC Location in IEEE 57-Bus System Using L-Index

The SVC is installed at the bus identified through the L-index method, which pinpoints the most voltage-sensitive buses in the IEEE 57-bus system. By targeting these critical locations, the SVC provides effective reactive power support, helping to maintain stable voltage profiles and improving the overall reliability and operational performance of the power network.

Journal of Information Systems Engineering and Management
2024, 9(4)
e-ISSN: 2468-4376
https://www.jisem-journal.com/

Research Article

Table 7 presents the HHO-based OPF results for the IEEE 57-bus system under both base and 11–43 contingency conditions, with and without SVC. The inclusion of SVC reduces voltage deviation and active power losses in both scenarios, while slightly decreasing fuel cost. Additionally, the total real power generation remains stable, and the MOF values indicate improved system efficiency and enhanced stability when SVC is applied.

For the IEEE 57-bus system, the SVC operates at 0.245 ∠ −82.76° pu under normal conditions, offering adequate reactive support to sustain voltage balance and stable power flow. When a contingency occurs, the rating increases to 0.4575 ∠ −87.34° pu, allowing the device to deliver stronger compensation, mitigate instability, and improve the overall security of the grid during disturbances.

This analysis highlights that in both IEEE 30-bus and IEEE 57-bus systems, the SVC ensures reliable performance under normal conditions while playing a crucial role in strengthening grid resilience during contingencies. By dynamically adjusting its reactive output, the SVC improves voltage stability, reduces system losses, and enhances the robustness of power system operation.

Table 7. HHO-OPF Results for IEEE 57-Bus System with and Without SVC Under Base and Contingency Conditions

	HHO excluding SVC	HHO with SVC at bus no: 31	HHO excluding SVC for 11-43 Contingency	HHO with SVC for 11-43 Contingency at bus no 42
G1(MW)	251.99	241.989	574.99	248.99
G2(MW)	78.05	81.99	99.9766	75.9766
G3(MW)	64.99	78.99	84.3622	78.32
G6(MW)	71.9	88.9	9.94536	88.98766
G8(MW)	465.88	447.19	78.4384	459.88
G9(MW)	199.5	199.5	199.5	199.5
G12(MW)	109.943	102.49	198.7018	90.99
Total real power generation (MW)	1242.253	1241.049	1245.91436	1242.64426
Fuel cost ($/hr)	46327	45986	50284	49028
Active losses (MW)	46.453	45.249	50.11436	46.84426
Voltage deviation (p.u)	5.593	3.496	7.678	3.748
MOF value	6982.4	6930.09	7578.83	7387.55

Critical Line Identification and TCSC Placement

The analysis indicates that the 8–9 transmission line has a HI of 0.59175, reflecting substantial stress under normal operating conditions. In the event of an N−1 contingency due to the outage of line 11–41, the 41–42 transmission line exhibits the highest HSI of 0.71409, identifying it as the most critical element in the network under this scenario. These results highlight the need for strategic placement of a TCSC to reinforce weak buses and heavily loaded lines, thereby improving voltage stability and overall system security. Table 8 presents HHO-based OPF outcomes for the IEEE 57-bus system with and without TCSC. In the base case, HHO without TCSC yields a total real power generation of 1242.253 MW, active losses of 46.453 MW, voltage deviation of 5.593 p.u., and fuel cost of $46,327/hr. Installing TCSC at line 8–9 improves these values to 1240.909 MW, 45.109 MW, 5.365 p.u., and $45,924/hr, respectively. During the 41–42 line contingency, HHO without TCSC records

Journal of Information Systems Engineering and Management
2024, 9(4)
e-ISSN: 2468-4376
https://www.jisem-journal.com/

Research Article

1244.724 MW, 48.924 MW, 6.412 p.u., and $49,109/hr, while with TCSC, the system achieves 1241.834 MW, 46.034 MW, 5.736 p.u., and $48,315/hr, demonstrating enhanced stability and operational efficiency.

In the IEEE 30-bus system, the TCSC provides effective series compensation with a normal operating rating of Ptcsc = 0.44681 pu and Qtcsc = 0.17289 pu at a reactance of X = 0.02 pu. These parameters enhance the transfer capability of transmission lines and contribute to maintaining bus voltage stability under steady-state conditions without imposing undue stress on the device. During contingency scenarios, the TCSC modifies its performance with Ptcsc = 0.4921 pu and Qtcsc = 0.1113 pu while keeping the same reactance, thereby increasing active power delivery and adjusting reactive power exchange to alleviate network stress and sustain stability. In the case of the IEEE 57-bus system, the TCSC under normal operation functions with Ptcsc = 0.612 pu, Qtcsc = 0.203 pu, and a reactance of X = 0.0523 pu, ensuring consistent reactive and active power support in the larger network. Under contingency conditions, its settings improve to Ptcsc = 0.738 pu, Qtcsc = 0.158 pu, and an effective reactance of X = 0.4872 pu, delivering stronger series compensation to redirect power flows, control voltage instability, and support post-fault recovery. This comparative analysis highlights that in both networks, the TCSC not only ensures stable operation under normal circumstances but also significantly strengthens stability, reliability, and resilience when optimized for contingencies.

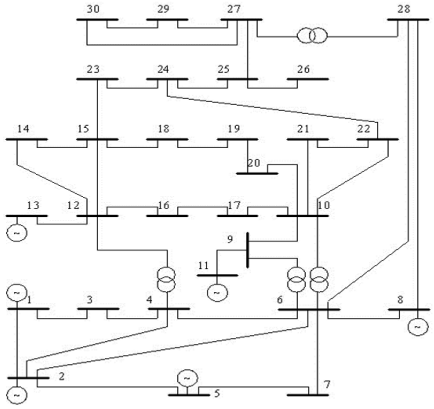

Figure 10. IEEE 30 Bus system Line Diagram

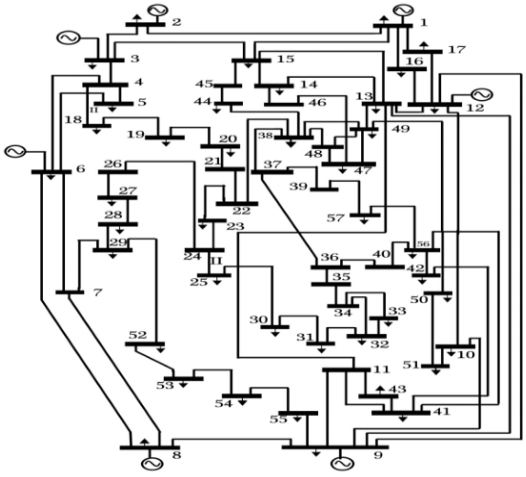

Figure 11. IEEE 57 Bus system Line Diagram

Journal of Information Systems Engineering and Management
2024, 9(4)
e-ISSN: 2468-4376
https://www.jisem-journal.com/

Research Article

Table 8: HHO-OPF Results for IEEE 57-Bus System with and Without TCSC Under Base and Contingency Conditions

	HHO excluding TCSC	HHO with TCSC at Line No 8-9	HHO excluding TCSC for Line No 41-42 Contingency	HHO with TCSC for Line No 41-42 Contingency
G1(MW)	251.99	249.989	261.99	263.886
G2(MW)	78.05	78.23	81.9766	78.3366
G3(MW)	64.99	75.19	80.99	74.99
G6(MW)	71.9	88.9	86.39766	71.98766
G8(MW)	465.88	461.88	439.88	465.88
G9(MW)	199.5	199.5	199.5	199.5
G12(MW)	109.943	87.22	93.99	87.254
Total real power generation (MW)	1242.253	1240.909	1244.72426	1241.83426
Fuel cost ($/hr)	46327	45924	49109	48315
Active losses (MW)	46.453	45.109	48.92426	46.03426
Voltage deviation (p.u)	5.593	5.365	6.412	5.736
MOF value	6982.4061	6920.98105	7401.558782	7280.33438

6. CONCLUSION

This work develops a multi-objective OPF approach to improve the efficiency, stability, and reliability of power systems, demonstrated on both the IEEE 30-bus and 57-bus systems. The proposed model addresses generation cost, active power losses, voltage deviation, and generator reallocation simultaneously, providing a comprehensive framework for system optimization. The HHO algorithm successfully solved the multi objective OPF, showing better convergence, robustness, and solution quality compared to the GA. Through N−1 contingency analysis, critical buses and transmission lines were identified in both networks, indicating locations prone to voltage instability. Based on the HI, the optimal placement of FACTS devices UPFC, TCSC, and SVC was determined, which effectively mitigated congestion and enhanced voltage profiles. The integration of generator reallocation with FACTS devices resulted in lower power losses, improved voltage stability, and stronger system resilience under normal and contingency conditions. These results demonstrate that combining intelligent optimization with advanced control devices significantly enhances power system performance across different network scales.

REFERENCES:

1. **Aghaei, J., Gitizadeh, M., Kaji, M.,** (2012) Placement and operation strategy of FACTS Devices Using Optimal Continuous Power Flow, Scientia Iranica, , Volume 19, No. 6, pp. 1683–1690.
2. **Anju Gupta, P R Sharma,** (2013) “Static and Transient Stability Enhancement of Power System by Optimally Placing UPFC”, Third International Conference on Advanced Computing &Communication Technologies, pp. 121-125.

3. **A.R Jordehi and Mahmood Joorabian,** (2011) "Optimal Placement of Multi-Type FACTS Devices in Power Systems Using Evolution Strategies", The 5th International Power Engineering and Optimization Conference (PEOCO2011), Malaysia, 6-7 June, pp. 352-357.
4. **Ali Ghasemi, Khalil Valipour, and Akbar Tohidi,** (2014) "Multi objective optimal reactive power dispatch using a new multi objective strategy", Electrical Power and Energy Systems, vol. 57, pp. 318–334.
5. **Abhishek Rajan, and T. Malakar**, (2015) "Optimal reactive power dispatch using hybrid Nelder–Mead simplex-based firefly algorithm", Electrical Power and Energy Systems, vol. 66, pp. 9–24.
6. **A. M. Shaheen, R. A. El-Sehiemy, and S. M. Farrag, (**2017) "Optimal reactive power dispatch using backtracking search algorithm," Australian Journal of Electrical and Electronics Engineering, vol. 13, no. 3, pp. 200–210.
7. **Anastasios G. Bakirtzis, Pandel N. Biskas, Christoforos E. Zoumas and Vasilios Petridis**, (2002) "Optimal Power Flow by Enhanced Genetic Algorithm", IEEE transactions on power systems, MAY 2002, VOL. 17, NO. 2, pp.229-236.
8. **Belyaev, N. A., Korovkin, N. V., Chudny, V. S., Frolov, O. V.,(** 2015**)** Reduction of Active Power Losses in Electric Power Systems with Optimal Placement of FACTS Devices, Young Researchers in Electrical and Electronic Engineering Conference (EIConRusNW), IEEE NW Russia, St. Petersburg, , pp. 150 – 154.
9. **B. Bhattacharyya and S. Raj,** (2016) "Swarm intelligence-based algorithms for reactive power planning with Flexible AC transmission system devices," International Journal of Electrical Power & Energy Systems, vol. 78, pp. 158 164.
10. **B. Bhattacharyya and N. Karmakar, (2020)** "Optimal Reactive Power Management Problem: A Solution Using Evolutionary Algorithms," IETE Technical Review, vol. 37, no. 5, pp. 540–548, 2020.
11. **Chang,C.S., and Huang,J.S.,(**1998**)** Worst-case Identification of Reactive Power Margin and Local Weakness of Power Systems, Electric Power Systems Research, , Vol.44, No. 2, pp. 77-83.
12. **Cui-Ru Wang, He-Jin Yuan, Zhi-Qiang Huang, Jiang-Wei Zhang and Chen-Jun Sun,** (2005) "A modified particle swarm optimization algorithm and its application in optimal power flow problem", in 4th International Conference on Machine Learning and Cybernetics, Guangzhou, August, pp .2885-2889.
13. **David E. Goldberg, (**1989**)** "Genetic Algorithms in Search, Optimization and Machine Learning", Reading, Mass., Addison Wesely, January 11.
14. **Dommel, H., & Tinney, W. (1968)**. Optimal power flow solutions. IEEE Transactions on Power Apparatus and Systems, PAS-87(10), 1866–1876. https://doi.org/10.1109/tpas.1968.292150
15. **El-Azab, M., Omran, W. A., Mekhamer, S. F., & Talaat, H. E. A**. (2020). Allocation of FACTS devices using a probabilistic multi-objective approach incorporating various sources of uncertainty and dynamic line rating. IEEE Access, 8, 167647–167664. https://doi.org/10.1109/access.2020.3023744
16. **Ela, A. a. E., Abido, M., & Spea, S**. (2010). Optimal power flow using differential evolution algorithm. Electric Power Systems Research, 80(7), 878–885. https://doi.org/10.1016/j.epsr.2009.12.018
17. **Geem, Zong Woo, Joong Hoon Kim, and G. V. Loganathan (**2001**)** "A new heuristic optimization algorithm: harmony search" Simulation, , Vol. 76, No.2, pp.60-68.
18. **Gao, B., Morison, G.K. and Kundur, P**., (1992) Voltage Stability Evaluation using Modal Analysis, IEEE Trans. on Power systems, , Vol.7 No. 4, pp. 1529-1542.

19. **Gerbex, S., Cherkaoui, R., and Germond**, A.J., (2001) Optimal Location of Multi-Type FACTS Devices in a Power System by Means of Genetic Algorithms, IEEE Trans. on Power Systems, Vol.16, No.3, pp. 537- 544.
20. **Galiana, F.D., Almeida, k., Toussaint, M., Griffin, J**., (1996) Assessment and Control of the Impact of FACTS Devices on Power System Performance, IEEE Trans on Power Systems, , Vol. 11, No. 4, pp. 1931-1936.
21. **Gotham, D., & Heydt, G.** (1998). Power flow control and power flow studies for systems with FACTS devices. IEEE Transactions on Power Systems, 13(1), 60–65. https://doi.org/10.1109/59.651614
22. **I Pisica, C. Bulac, L. Toma, M. Eremia**, (2009) "Optimal SVC Placement in Electric Power Systems Using a Genetic Algorithms Based Method", IEEE Bucharest Power Tech Conference, June 28th - July 2nd, Bucharest, Romania, pp.1-6.
23. **Jayasankara,V., Kamaraj, N., Vanaja,N**.,(2010) Estimation of Voltage Stability Index for Power System Employing Artificial Neural Network Technique and TCSC Placement, Neurocomputing, , , Vol. 73, pp. 3005–3011.
24. **Jurado.F and J.A. Rodriguez**, (1999) "Optimal Location of SVC based on System Loadability and Contingency Analysis", Proceedings of the 7th IEEE International Conference on Emerging Technologies and Factory Automation, , Vol. 2, PP. 1193 – 1199.
25. **Krishnan, V., McCalley,J. D.**, (2012) Contingency Assessment Under Uncertainty for Voltage Collapse and its Application in Risk Based Contingency Ranking, Electrical Power and Energy Systems, ,Vol.43, pp. 1025–1033.
26. **Kumar,G. N., Kalavathi.,M. S**., (2014) Cat Swarm Optimization for Optimal Placement of Multiple UPFC's in Voltage Stability Enhancement Under Contingency, Electrical Power and Energy Systems, , Vol. 57, pp. 97–104.
27. **Kumar,B. V., Srikanth,N.V.,** (2015) Optimal Location and Sizing of Unified Power Flow Controller (UPFC) to Improve Dynamic Stability: A Hybrid Technique, Electrical Power and Energy Systems, , Vol. 64, pp. 429–438.
28. **Kazemi,A. and Badrzadeh,B**., (2004) Modeling and Simulation of SVC and TCSC to Study Their Limits on Maximum Load ability Point, International Journal of Electrical Power & Energy Systems, Volume 26, No. 8, pp. 619- 626.
29. **Santhosh Kasi1* and R Neela2** (2021) Harris hawks' optimization algorithm-based power loss minimization in micro grid incorporated with distributed generation. IOP Conf. Series: Materials Science and Engineering. ICRIET 2020. 1070 (2021) 012099.
30. **Ali Asghar Heidaria,b, Seyedali Mirjalilic, Hossam Farisd, Ibrahim Aljarahd, Majdi Mafarjae, Huiling Chenf,*(** 2019)Harris hawks optimization: Algorithm and applications Future Generation Computer Systems Volume 97, August 2019, Pages 849-872